Journal of Physiology (1991), **435**, *pp.* 83–99
With 8 figures
Printed in Great Britain

EFFECTS OF EXTERNAL AND INTERNAL K^+ IONS ON MAGNESIUM BLOCK OF INWARDLY RECTIFYING K^+ CHANNELS IN GUINEA-PIG HEART CELLS

BY HIROKO MATSUDA

From the Department of Physiology, Faculty of Medicine, Kyushu University, Fukuoka 812, Japan

(*Received 12 March 1990*)

SUMMARY

1. Block of the inwardly rectifying K^+ channel by intracellular Mg^{2+} was studied in guinea-pig ventricular cells at varying external or internal K^+ concentrations. Sucrose or glucose was mainly used as a substitute for K^+.

2. The current–voltage (*I–V*) relation for the single channel, in the absence of internal Mg^{2+}, was almost linear in 30 mM-external K^+ and 150 mM-internal K^+ (30 mM $[K^+]_o$) and in 45 mM-internal K^+ and 150 mM-external K^+ (45 mM $[K^+]_i$) as well as in 150 mM-external and internal K^+ (the control condition). The channel conductance was $31{\cdot}7 \pm 1{\cdot}7$ pS (mean ± S.D., $n = 36$) in the control, $23{\cdot}1 \pm 1{\cdot}2$ pS ($n = 8$) in 30 mM $[K^+]_o$ and $29{\cdot}7 \pm 1{\cdot}3$ pS ($n = 16$) in 45 mM $[K^+]_i$, respectively.

3. Mg^{2+} on the cytoplasmic side blocked the outward currents without affecting the inward currents. Outward mean open-channel currents were measured at different Mg^{2+} concentrations (0–100 μM) and voltages. The current–voltage relation rectified inwardly in the presence of internal Mg^{2+} in a voltage- and concentration-dependent manner.

4. Outward mean open-channel currents were normalized to that measured in the absence of Mg^{2+}. The normalized current–voltage relation in 45 mM $[K^+]_i$ was almost superimposable on that obtained in the control at the same Mg^{2+} concentration, while that in 30 mM $[K^+]_o$ was shifted in the negative direction by some 30 mV.

5. The normalized current–Mg^{2+} concentration curve was fitted by a one-to-one binding curve at each K^+ condition and voltage. In a semilogarithmic plot of dissociation constant *versus* membrane potential, data points for 45 mM $[K^+]_i$ were located on the same line as the control, whereas data points for 30 mM $[K^+]_o$ were shifted in the negative direction by about 30 mV. The dissociation constant at 0 mV is 37 μM in the control and 45 mM $[K^+]_i$ and 8·8 μM in 30 mM $[K^+]_o$. The voltage dependence of dissociation constants gives a value for the fractional electrical distance of the Mg^{2+} binding site of 0·57.

6. Subconductance levels with one-third and two-thirds of the unitary amplitude were seen with low internal Mg^{2+} at 45 mM $[K^+]_i$ or 30 mM $[K^+]_o$ as well as in the control condition. Blocking and unblocking rates were calculated on the assumption that the channel is composed of three identical conducting units and each unit is

MS 8343

blocked by Mg^{2+} independently. An increase in the blocking rate was more evident than a decrease in the unblocking rate with reduction of external K^+.

7. The results are considered in terms of a three-barrier, two-site ionic permeation model. Dependence of the dissociation constant at 0 mV on the external K^+ implies that the depth of the energy well for Mg^{2+} is affected by external K^+. Such an assumption is needed to reproduce the shift of the block comparable to the change in the zero-current potential when external K^+ is changed.

INTRODUCTION

Most cardiac K^+ channels show inward-going rectification, permitting a greater entry of K^+ under hyperpolarization than exit under depolarization. This behaviour plays an important role in maintaining the long-lasting action potential characteristic of cardiac cells. The mechanism by which such rectification might occur has remained a puzzle for close to 40 years since it was first reported in the resting K^+ conductance of skeletal muscle (Katz, 1949). Recently, however, evidence has accumulated from several cardiac K^+ channels that voltage-dependent block by internal Mg^{2+} causes the inward rectification: in the inwardly rectifying K^+ channels (Matsuda, Saigusa & Irisawa, 1987; Vandenberg, 1987; Matsuda, 1988), in the adenosine 5′-triphosphate (ATP)-regulated K^+ channels (Findlay, 1987; Horie, Irisawa & Noma, 1987), in the muscarinic receptor-operated K^+ channel (Horie & Irisawa, 1987, 1989) and in the Na^+-activated K^+ channel (Wang, Kimitsuki & Noma, 1991).

In comparison, the characteristic findings in the Mg^{2+} block of the inwardly rectifying K^+ channel are that Mg^{2+} is effective at much lower concentrations and that substate behaviour is seen easily with internal Mg^{2+} at a micromolar level (Matsuda, 1988). The outward single-channel current fluctuates between four equally spaced conductance levels (including the zero-current level), suggesting that the cardiac inwardly rectifying K^+ channel consists of three identical conducting units. They usually function co-operatively to form a single channel, but Mg^{2+} can enter and plug up each subunit to produce the substate behaviour at positive potentials.

To obtain further information on the mechanism of rectification, the effects of external and internal K^+ on the Mg^{2+} block were studied. In comparison to 150 mM-symmetrical K^+ controls, Mg^{2+} block at a given membrane potential was potentiated by reducing the external K^+, while it was little affected by reducing the internal K^+. The results are considered in terms of a three-barrier, two-site ionic permeation model.

METHODS

Preparations. Guinea-pigs were anaesthetized with intraperitoneal injections of sodium pentobarbitone (30 mg/kg) and the chest was opened under artificial respiration. The ascending aorta was cannulated *in situ* and the heart was dissected out. The blood was washed out by coronary perfusion with Tyrode solution equilibrated with 100 % O_2. The compositions of the main solutions are listed in Table 1. After the heart was perfused with about 50 ml of Ca^{2+}-free Tyrode solution, the perfusate was switched to a Ca^{2+}-free Tyrode solution containing 0·4 mg/ml collagenase (Sigma, type I), 0·4 mg/ml trypsin inhibitor (Sigma, type II-S) and 0·8 mg/ml bovine albumin (Sigma), which was recirculated with a peristaltic pump for about 30 min. Thereafter collagenase was washed out with 100 ml of a high-K^+ storage solution containing (in mM): KCl, 120; succinic acid,

TABLE 1. Composition of solutions (mM)

Bathing solution									
	NaCl	NaH_2PO_4	KCl	$CaCl_2$	$MgCl_2$	HEPES	Glucose	V_j (mV)	
Tyrode solution	144	0·33	5·4	1·8	0·5	5	5·5	0	
		Potassium aspartate	KCl	KH_2PO_4	$MgCl_2$	EDTA	K_2ATP	HEPES	V_j (mV)
150 mM-K^+, Mg^{2+}-free		60	65	1	0	5	3	5	−9·5
150 mM-K^+, Mg^{2+} test		60–65	65	1	1·01–3·85	2–5	3	5	−9·5
		Sucrose or glucose	KCl	KH_2PO_4	$MgCl_2$	EDTA	K_2ATP	HEPES	V_j (mV)
45 mM-K^+, Mg^{2+}-free		220	20	1	0	1–5	3–5	5	−10
45 mM-K^+, Mg^{2+} test		220	20	1	0·24–4·1	1–5	3–5	5	−10
Pipette solution									
	KCl	Sucrose	$CaCl_2$	HEPES	V_j (mV)				
150 mM-K^+	150	0	1	5	−2				
30 mM-K^+	30	240	1	5	−5·5				

The pH of the solutions was adjusted to 7·4 with KOH or NaOH (Tyrode solution). The K^+ concentrations after titration were approximately 155 mM in 150 mM-K^+ internal solution, 44–50 mM in 45 mM-K^+ internal solution, 152 mM in 150 mM-K^+ pipette solution and 32 mM in 30 mM-K^+ pipette solution.

The dipotassium salt of EDTA was used.

V_j was the liquid junction potential between the solution and the Tyrode solution. (Tyrode solution side was negative).

10; pyruvic acid, 5; $MgSO_4$, 5; taurine, 20; creatine, 5; HEPES, 10; glucose, 20; and ethyleneglycol-bis-(β-aminoethylether)N,N′-tetraacetic acid, 0·2; pH was adjusted to 7·3 with KOH. The temperature of all perfusates was kept at 36–37 °C during coronary perfusion, and the hydrostatic pressure for the perfusion was approximately 65 cmH_2O. Finally, the ventricles were cut and chopped with scissors. Gentle agitation of the chunks released the cells into the storage solution. The cells were filtered through a 150 μm mesh net and stored at 4 °C.

Recording techniques. Recordings of single-channel currents were performed using a heat-polished patch electrode (Hamill, Marty, Neher, Sakmann & Sigworth, 1981). Pipettes were made from capillaries of high-melting-temperature glass and were coated near their tips with silicone to reduce electrical capacitance. The electrode resistance ranged between 10 and 15 MΩ when filled with 150 mM-KCl pipette solution.

Current records illustrated in this paper were obtained from open cell-attached patches (Horie *et al*. 1987; Matsuda, 1988). After the giga-seal was attained in Tyrode solution, nominally Ca^{2+}-free Tyrode solution and then 150 mM-K^+, Mg^{2+}-free solution were perfused. The cell membrane was ruptured in the last solution by crushing the tip of another patch pipette (filled with the same solution as the bathing solution) against the cell on the glass bottom of the recording chamber. This procedure did not affect the giga-seal and the intracellular milieu was equilibrated with the bathing solution through the hole made in the membrane. The pipette used for rupture was withdrawn from the cell. ATP at a concentration of 3 mM suppressed the ATP-regulated K^+ channel. Thus the channel observed constantly under this condition was the inwardly rectifying K^+ channel responsible for the resting conductance. The channel activity in open cell-attached patches was maintained for as long as 30–60 min. The free Mg^{2+} concentration of the bathing solution was buffered using ethylenediamine tetraacetic acid (EDTA) according to Fabiato & Fabiato (1979) with a correction by Tsien & Rink (1980). The temperature of the solution in the chamber was kept at 24–25 °C.

Recordings were made with an EPC-7 patch clamp amplifier (List electronic). A steady potential was applied to the inside of the electrode to set the holding potential of the membrane patch, and outward currents were elicited by depolarizing steps of 130 ms every 1–2 s. Membrane potentials are expressed in the conventional way, inside relative to outside, and outward currents are ascribed a positive sign. The membrane potentials were corrected for the liquid junction potential at the tip of the patch pipette in Tyrode solution and also that at the tip of the indifferent reference electrode filled with Tyrode solution in the bathing solution.

Data analysis. Data were recorded on a video cassette (Victor, BR-6400) using a PCM converter system (NF, RP-880) and stored for subsequent computer analysis (NEC, PC-98 XL). Currents were filtered using a four-pole low-pass Bessel filter (NF, FV-665, 48 dB/octave) with a −3 dB corner frequency of 1·2 kHz and sampled every 0·2 ms, unless otherwise indicated. Capacitative and leakage currents were removed by the transient cancellation facility of the amplifier and by subtracting from each trace the average of current traces without events. Mean open-channel currents were calculated from twenty to fifty frames as follows. A threshold was set just above the zero-current level and data points below the threshold were averaged. The difference between each data point lying above the threshold and the averaged baseline was calculated, and the differences were integrated. The resulting integrated value was then divided by the duration of the channel opening. To measure the mean dwell time in each substate, current records with single-channel activity were reconstructed by setting a threshold level at around half of the open level of the subunits for discrimination of open and blocked states of subunits. The dwell-time histogram in each substate was formed from reconstructed traces and then fitted with an exponential function using a least-squares algorithm. Events of very short duration, too rapid to properly resolve, were excluded from the fitting by omitting the first bin. Average results throughout this paper are given as mean ± S.D.

RESULTS

I–V relation for the single channel in the absence of the internal Mg^{2+} with reduced external or internal K^+ concentration

As reported previously (Sakmann & Trube, 1984), outward single-channel currents through the inwardly rectifying K^+ channel are not recorded in the cell-attached configuration. Outward currents, however, appear in response to voltage steps or voltage ramps to levels more positive than the equilibrium potential for K^+ (E_K) when the internal surface of the cell is exposed to divalent cation-free, high-K^+ solution (Matsuda *et al.* 1987; Vandenberg, 1987; Matsuda, 1988). Figure 1 shows transient outward currents induced by voltage steps to levels more positive than E_K

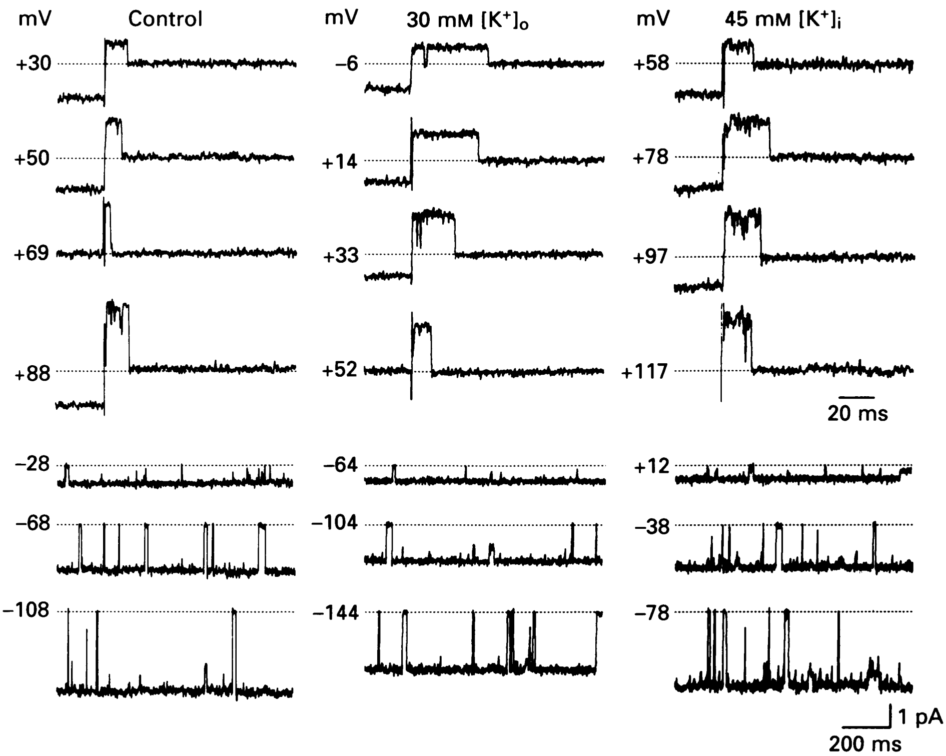

Fig. 1. Single-channel currents recorded from an inwardly rectifying K^+ channel in the open-cell-attached configuration at 150 mM external and internal K^+ (control), 30 mM-external and 150 mM-internal K^+ (30 mM $[K^+]_o$) and 150 mM-external and 45 mM-internal K^+ (45 mM $[K^+]_i$). Numbers to the left of each current trace refer to (upper four panels) the potential levels during the depolarizing steps from -48 mV (control), -84 mV (30 mM $[K^+]_o$) and -18 mV (45 mM $[K^+]_i$), or (lower three panels) holding potential. Currents of lower panels were filtered at 1 kHz and sampled every 1 ms. Capacitive and leakage currents were removed by the transient cancellation facility of the amplifier only in the current at $+117$ mV with 45 mM $[K^+]_i$. The holding current was removed in the records at $+69$ mV for the control and $+52$ mV for 30 mM $[K^+]_o$ by subtracting the average of the current traces with inward events but no outward events. The dotted line indicates zero-current level.

(upper panels) and inward currents recorded in a steady-state condition (lower panels), under conditions which vary the external and internal K^+ concentrations. E_K, predicted from transmembrane K^+ concentrations, is 0 mV with 150 mM external and internal K^+ (control), -39 mV with 30 mM-external K^+ and 150 mM-internal K^+ (30 mM $[K^+]_o$) and $+30$ mV with 150 mM-external K^+ and 45 mM-internal K^+ (45 mM $[K^+]_i$). Current records obtained at nearly the same driving force are arranged in the same row. Inward currents show long-lasting openings characteristic of the inwardly rectifying K^+ channel. When a depolarizing pulse was applied during the open state from a holding potential of -48 mV (control), -84 mV (30 mM $[K^+]_o$) and -18 mV (45 mM $[K^+]_i$), the channel stayed open at the onset of the pulse and closed during the pulse (130 ms in duration) in most cases. This

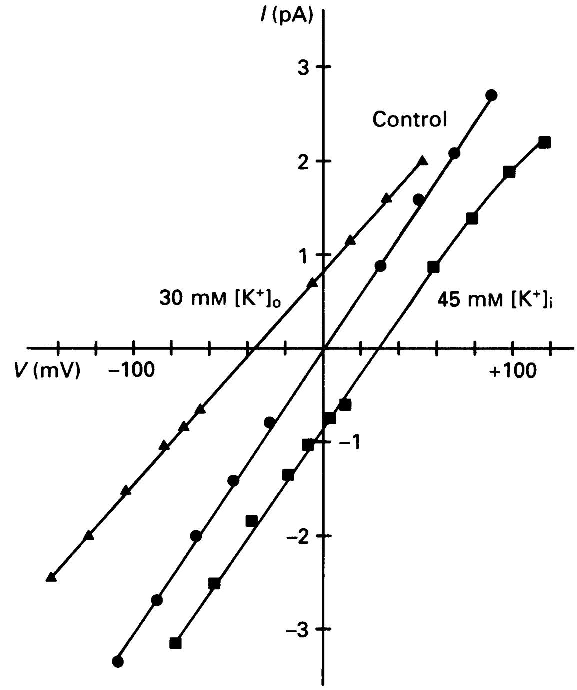

Fig. 2. Single-channel I–V relationships obtained from the same patches as in Fig. 1.

indicates that a voltage-dependent gating mechanism exists independently of the Mg^{2+} block: even in the absence of internal Mg^{2+}, the open-state probability is reduced at potentials more positive to E_K, resulting in inward rectification of the steady state (Matsuda *et al.* 1987; Matsuda, 1988).

The I–V relation was almost linear in the potential range examined in 30 mM $[K^+]_o$ and 45 mM $[K^+]_i$ as well as in the control, though in some cases a slight inward rectification was observed at very positive potentials in 45 mM $[K^+]_i$ (Fig. 2). The zero-current potential was $+0{\cdot}6 \pm 2{\cdot}1$ mV in the control ($n = 36$), $-34{\cdot}9 \pm 1{\cdot}8$ mV in 30 mM $[K^+]_o$ ($n = 8$) and $+27{\cdot}9 \pm 2{\cdot}3$ mV in 45 mM $[K^+]_i$ ($n = 16$). The shift of the zero-current potential is equivalent to 53 mV per tenfold change in both the external and internal K^+ concentrations. The single-channel conductance was $31{\cdot}7 \pm 1{\cdot}7$ pS in the control ($n = 36$), $23{\cdot}1 \pm 1{\cdot}2$ pS in 30 mM $[K^+]_o$ ($n = 8$) and $29{\cdot}7 \pm 1{\cdot}3$ pS in 45 mM $[K^+]_i$ ($n = 16$). The unitary conductance depends on the external K^+ more profoundly than on the internal K^+: the exponents of the K^+ dependence of the unitary conductance are 0·22 for external K^+ and 0·06 for internal K^+.

In the present work either sucrose or glucose was used as a substitute for internal K^+, as they were among the few substitutes which preserved the outward current (e.g. Tris ions at a concentration of 5 mM on the cytoplasmic side abolished the outward current). Sucrose was used as a substitute for external K^+, because it had the least effect on the inward current among the substances tested. As in skeletal muscle (Matsuda & Stanfield, 1989), external Na^+ decreased the open time of the inward current without affecting the current amplitude, while choline, Tris and

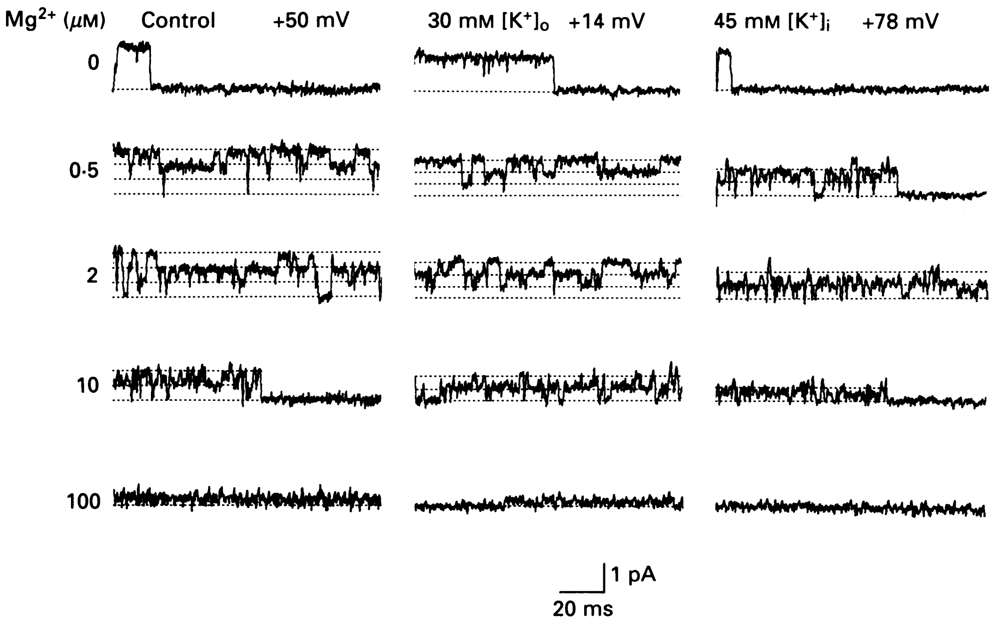

Fig. 3. Effect of internal Mg^{2+} on the outward single-channel current. After recording the control trace in each patch, while perfusing the open cell with Mg^{2+}-free solution, the Mg^{2+} concentration of the perfusing solution was increased progressively. The dotted lines show, from the bottom, current levels for the zero, one-third, two-thirds and fully open channel. (It is the same in the following figure.)

tetramethylammonium (TMA) in the pipette reduced the amplitude of inward unitary currents without affecting the amplitude of outward unitary currents or kinetics. As control experiments, I examined the effect of low external K^+ on the Mg^{2+} block using choline and TMA ions and obtained a similar result as with sucrose (see below). Thus, although non-charged substitutes introduced asymmetric changes in ionic strength, it is unlikely that use of non-charged substitutes caused the present results, at least for external K^+ experiments.

Comparison of Mg^{2+} block at different K^+ concentrations

As mentioned in the previous section, the conductance of the inwardly rectifying K^+ channel is ohmic and the channel closes on depolarization above E_K because of the voltage-dependent gating kinetics, thus causing steady-state inward rectification. An additional mechanism responsible for the rectification of this channel is the voltage-dependent block of the channel by intracellular Mg^{2+} (Matsuda *et al.* 1987; Vandenberg, 1987; Matsuda, 1988).

Figure 3 shows the outward current during clamp pulses to $+50$ mV from a holding potential of -48 mV (control), to $+14$ mV from -84 mV (30 mM $[K^+]_o$) and to +78 mV from −18 mV (45 mM $[K^+]_i$). The potential level during the steps corresponds to a driving force of some +50 mV in each case. In the absence of internal Mg^{2+}, full-size single-channel currents were induced on depolarization, usually followed by a closed state during 130 ms pulses. With Mg^{2+} at a micromolar

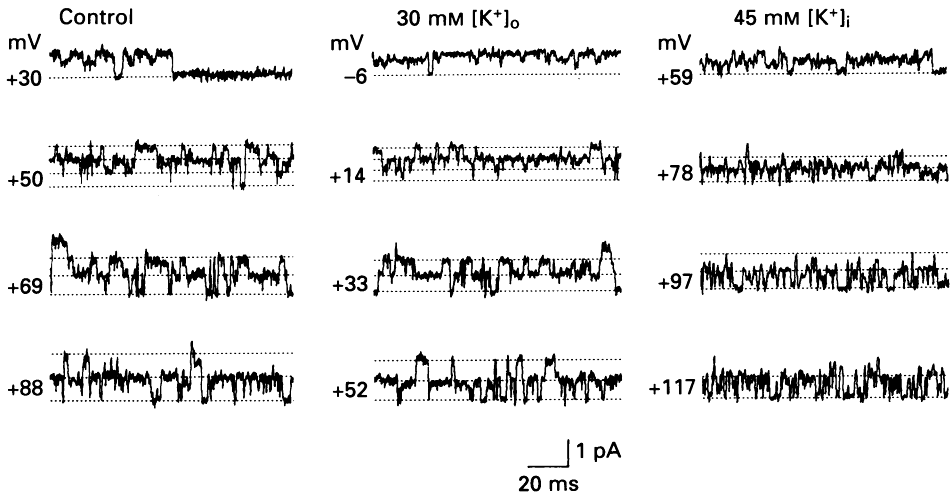

Fig. 4. Outward currents at different voltages in the presence of 2 μM-internal Mg^{2+}. Transitions could be observed between well-defined sublevels. The same patches as in Fig. 3.

level, the outward open-channel currents showed sublevels with one-third and two-thirds of the unit amplitude and fluctuated between sublevels. As the Mg^{2+} concentration was increased, the channel stayed at the lower levels more frequently and fluctuations became faster. The outward current became noisy in the presence of 100 μM-Mg^{2+}.

As in the control, sublevels with one-third and two-thirds of the unit amplitude were observed in 30 mM $[K^+]_o$ or 45 mM $[K^+]_i$. Note the levels at which the current resides and the rate of fluctuations between sublevels. Compared at the same Mg^{2+} concentration and driving force, the extent of the block in 30 mM $[K^+]_o$ seems similar to that in the control, while the outward currents were blocked more extensively in 45 mM $[K^+]_i$ than in the control.

As may be anticipated from experiments with other blocking ions, blockage by internal Mg^{2+} increases both with depolarization of the membrane and with the concentration of Mg^{2+}. Figure 4 shows outward current records at different voltages in the presence of 2 μM-Mg^{2+}. Traces recorded at nearly the same driving force are arranged in the same row. In each column, as voltage is made increasingly positive, the probability of observing the lower levels increases progressively, while that of observing the higher levels decreases. Compared at the same driving force, the outward current in 30 mM $[K^+]_o$ stayed at similar levels to those in the control. On the other hand, the outward current in 45 mM $[K^+]_i$ stayed at lower levels than in the control. From a different point of view, compared at the same potential (e.g.

+50 mV in the control and +52 mV in 30 mM $[K^+]_o$), the outward current stayed at lower levels with low external K^+, indicating that the Mg^{2+} block was potentiated by reducing external K^+. A difference in the test potential of some 10 mV made it difficult to compare the block between the control and 45 mM $[K^+]_i$ at the same

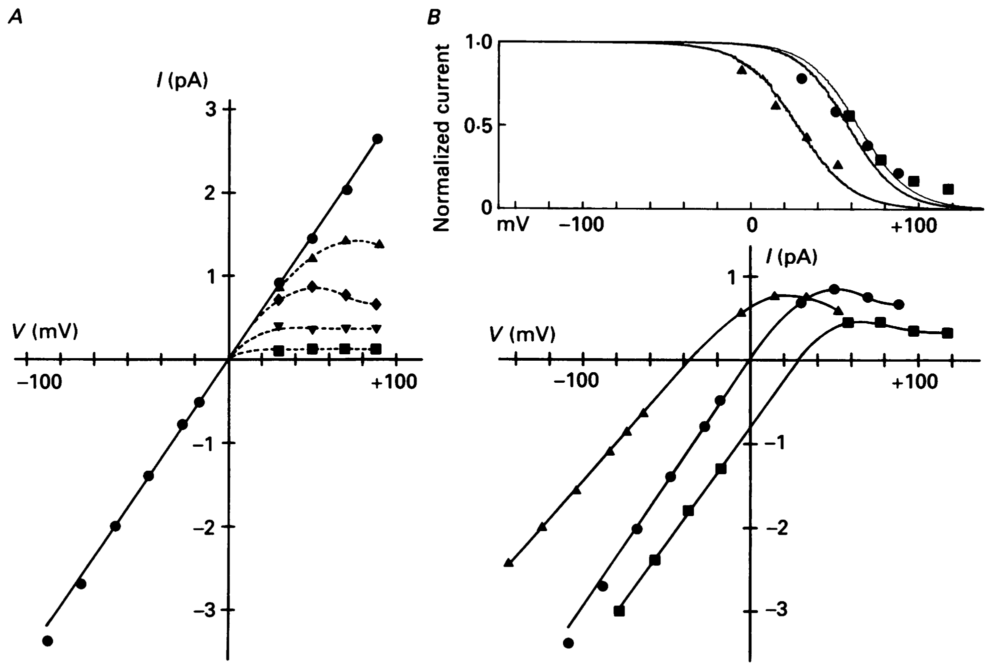

Fig. 5. *A*, mean open-channel current–voltage relationship in the control K^+ condition at a Mg^{2+} concentration of 0 (●), 0·5 (▲), 2 (◆), 10 (▼) and 100 (■) μM. The slope conductance was increased slightly at more negative potentials than −80 mV. *B*, normalized current–voltage (upper panel) and mean open-channel current–voltage relationships (lower panel) in the presence of 2 μM-Mg^{2+}. ●, control; ▲, 30 mM $[K^+]_o$; ■, 45 mM $[K^+]_i$. Curves in the upper panel represent theoretical curves based on the three-barrier, two-site ionic permeation model described in the Discussion for (from left) 30 mM $[K^+]_o$, control and 45 mM $[K^+]_i$.

potential. It will be shown in the next section that the extent of the block is similar to that in the control.

I–V relations under the Mg^{2+} block

To quantify the blocking effect of Mg^{2+} at different K^+ conditions, outward mean open-channel currents were calculated from twenty to fifty frames. Zero-current periods longer than 10 ms have been attributed to the closed state of the channel and excluded from the analysis. Unitary amplitudes were measured for inward currents. Figure 5*A* shows the *I–V* relations at different Mg^{2+} concentrations (0–100 μM) in the control K^+ condition. In the presence of internal Mg^{2+}, the chord conductance was decreased at potentials positive to E_K. Depression of the outward current was increased with increasing Mg^{2+} concentration and depolarization.

I–V relations with 2 μM-Mg^{2+} at different K^+ concentrations are shown in the lower panel of Fig. 5B. The curves for the control and 30 mM $[K^+]_o$ cross each other at around +30 mV. At more positive voltages, the current amplitude in the control is larger than that with 30 mM $[K^+]_o$. The amplitude of the peak of the I–V curve

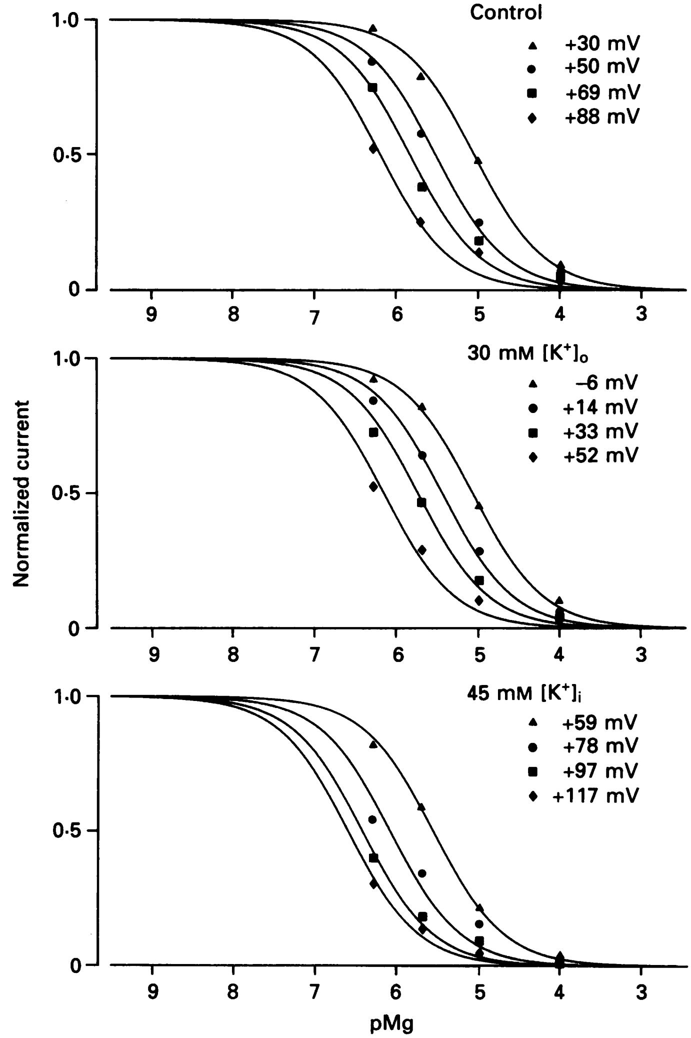

Fig. 6. Normalized current–concentration curves obtained from the data shown in Fig. 5. Each curve was fitted by a one-to-one binding curve.

decreases in the order of control, 30 mM $[K^+]_o$ and 45 mM $[K^+]_i$. The mean open-channel current was normalized to that in the absence of Mg^{2+} and plotted against the membrane potential in the upper panel of Fig. 5B. The data at 45 mM $[K^+]_i$ and the control are closely related to each other, indicating that the blocking effect of Mg^{2+} at a given voltage was little affected by reducing internal K^+. On the other hand, the relation is shifted in the negative direction by some 30 mV with 30 mM

$[K^+]_o$, i.e. the blocking effect increases with low external K^+ when compared at a fixed voltage. The shift of some 30 mV is a little smaller than that of the zero-current potential, but is nearly the same.

The normalized current values of 0·56 at +20 mV and 0·40 at +38 mV were obtained when 120 mM-KCl in the pipette solution was replaced with equimolar choline chloride; and the values 0·60 at +20 mV and 0·45 at +38 mV were obtained when KCl was replaced with TMA-Cl. These values compare well with sucrose data observed in Fig. 5*B*. Thus the shift of the block was similar irrespective of whether a substitute for external K^+ was charged or not.

Dissociation constants in the Mg^{2+} block

Figure 6 shows normalized current–Mg^{2+} concentration relations at different voltages and K^+ concentrations. The data for nearly the same driving force are presented by the same symbol. The results give a reasonable fit to concentration–effect curves predicted by assuming one-to-one binding of Mg^{2+} to a receptor.

In a semilogarithmic plot of dissociation constant (averaged in three to four experiments) *versus* membrane potential, data points at each K^+ condition can be fitted by a straight regression line, indicating that the dissociation constant decreases exponentially as the membrane potential is increased (Fig. 7). Furthermore data for the control and 45 mM $[K^+]_i$ seem to be fitted by the same line, though there is some deviation. The line fitted to the data at 30 mM $[K^+]_o$ parallels this some 30 mV apart. The dissociation constants were 4·3 μM at +20 mV and 2·1 μM at +38 mV when external K^+ was replaced with TMA-Cl, suggesting that a parallel shift was also induced with a charged substitute.

The dissociation constant (K_D) is described as:

$$K_D(V) = K_D(0)\exp(-z\delta VF/RT),$$

where V is membrane potential, z the valency of the blocking ion, and δ the fractional electrical distance between the internal mouth of the aqueous pore and the Mg^{2+} binding site (Woodhull, 1973). F, R and T have their usual meaning. The slope of the regression lines gave a values of 0·57 for δ. The value of K_D at 0 mV, K_D (0), is independent of the internal K^+ (37 μM for the control and 45 mM $[K^+]_i$), but is dependent on the external K^+ (8·8 μM for 30 mM $[K^+]_o$).

Mechanism of relief of the Mg^{2+} block by external K^+

The above results indicate that the block by intracellular Mg^{2+} is increased by decreasing the external K^+, i.e. the Mg^{2+} block is relieved by increasing the external K^+ concentration. There are two possible mechanisms for relief: first, that K^+ relieves block by competing for the saturable Mg^{2+} binding site in the aqueous pore; and second, that K^+ ions speed the exit of blocking Mg^{2+} ions. To distinguish between these two classes of mechanisms, the substate behaviour seen with low internal Mg^{2+} was analysed, and blocking and unblocking rates were calculated on the basis of a binomial scheme (Matsuda, 1988).

As shown in Figs 3 and 4, the outward open channel showed, in the presence of internal Mg^{2+} at a micromolar level, sublevels with one-third and two-thirds of the unit amplitude and fluctuated between four levels including the fully open channel current and the zero-current levels. Previous work showed that the open-state occupancies of each current level are in reasonable agreement with the binomial theorem. This suggests that the inwardly rectifying K^+ channel is composed of three

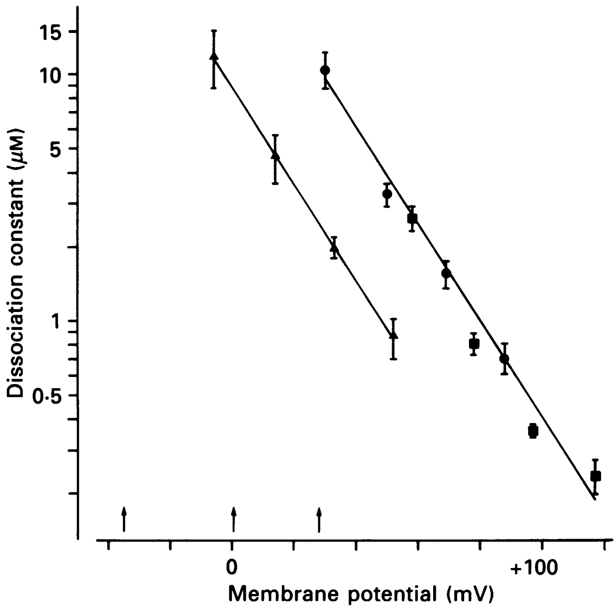

Fig. 7. Dependence of the dissociation constant on membrane potential. ●, control; ▲, 30 mM $[K^+]_o$; ■, 45 mM $[K^+]_i$. The bars give ±S.D of means. Dissociation constants (n = 3–4) are: 10·5±1·7 μM at +30 mV, 3·2±0·3 μM at +50 mV, 1·6±0·2 μM at +69 mV and 0·70±0·10 μM at +88 mV in the control; 11·9±3·2 μM at −6 mV, 4·6±1·0 μM at +14 mV, 2·0±0·2 μM at +33 mV and 0·87±0·16 μM at +52 mV in 30 mM $[K^+]_o$; and 2·6±0·3 μM at +59 mV, 0·81±0·08 μM at +78 mV, 0·32±0·08 μM at +97 mV and 0·24±0·04 μM at +118 mV in 45 mM $[K^+]_i$. In a semilogarithmic plot, data for the control and 45 mM $[K^+]_i$ were fitted by a straight line in parallel with that fitted to data at 30 mM $[K^+]_o$. The slope of the regression lines gave the fractional electrical distance of the Mg^{2+} binding site, $\delta = 0{\cdot}57$. Arrows just above the voltage axis indicate the averaged zero-current potential at (from left) 30 mM $[K^+]_o$, control and 45 mM $[K^+]_i$.

identical conducting subunits and each subunit is blocked by Mg^{2+} independently. Sublevels with one-third or two-thirds of the unit amplitude are also induced in the inward current by the external application of Cs^+ or Rb^+, though the effect is not as consistent as in the case of Mg^{2+} block (Matsuda, Matsuura & Noma, 1989).

The kinetic properties of blockage associated with substate behaviour were studied based on a binomial scheme (Matsuda, 1988; Matsuda *et al.* 1989). If the block of each subunit is described as:

$$\mathrm{O} \underset{\lambda}{\overset{\mu}{\rightleftharpoons}} \mathrm{B},$$

where O and B are the open and blocked states of each subunit, λ is the first-order unblocking rate and μ the second-order blocking rate, the open-state probability of

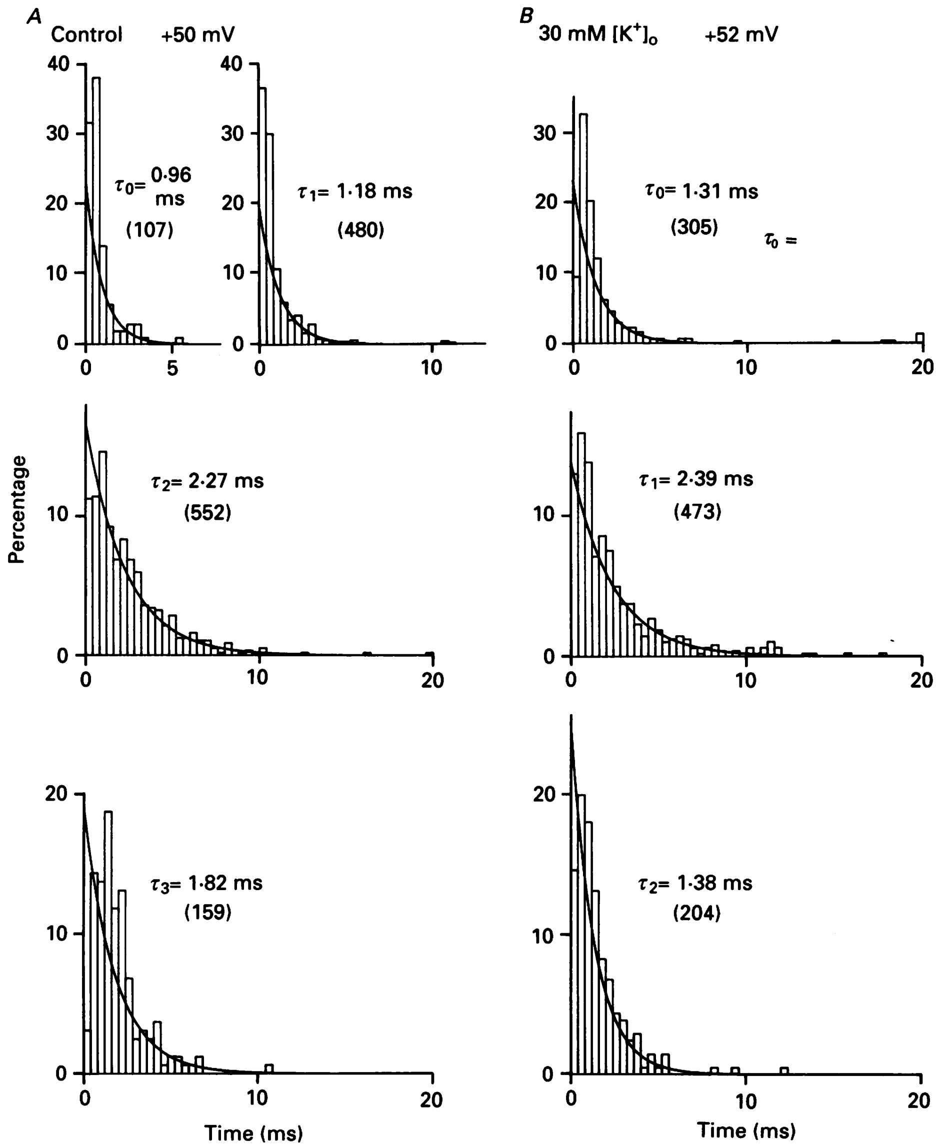

Fig. 8. Dwell-time histograms in each substate for the control (*A*) and 30 mM $[K^+]_o$ (*B*). The histograms were formed in 0·4 ms bins and fitted with a single-exponential function with the time constants (τ) indicated. The numbers of events are shown in parentheses. Estimation of τ_3 from the dwell-time histograms was difficult because of the small number of events (41) at 30 mM $[K^+]_o$. Its mathematical average was 1·39 ms.

the subunits, p, is expressed as $\lambda/(\lambda+\mu)$ and transitions between substates during the open state of the channel can be described as:

$$O_3 \underset{\lambda}{\overset{3\mu}{\rightleftharpoons}} O_2 \underset{2\lambda}{\overset{2\mu}{\rightleftharpoons}} O_1 \underset{3\lambda}{\overset{\mu}{\rightleftharpoons}} O_0,$$

where O_0, O_1, O_2 and O_3 are the substates in which all, two, one and none of three subunits are blocked, respectively. In this scheme, the mean dwell times in the substates are given as:

$$1/\tau_0 = 3\,\lambda,$$

$$1/\tau_1 = 2\,\lambda + \mu,$$

$$1/\tau_2 = \lambda + 2\,\mu,$$

and

$$1/\tau_3 = 3\,\mu,$$

where τ_0, τ_1, τ_2 and τ_3 represent the mean lifetimes in O_0, O_1, O_2 and O_3, respectively.

Dwell-time histograms in each substate with 2 μM-Mg^{2+} were compiled from reconstructed traces (Fig. 8). They could be fitted by single-exponential functions with the time constants indicated. Under the influence of Mg^{2+}, the fully open state was not observed frequently, so that it was difficult to estimate τ_3 from the dwell-time histogram in some cases. λ and μ were calculated from τ_2 and the normalized current amplitude, which should be equivalent to p: 179·5 and 130·5 s^{-1} for the control at +50 mV (Fig. 8*A*) and 122·4 and 301·1 s^{-1} for 30 mM $[K^+]_o$ at +52 mV (Fig. 8*B*). Values of λ and μ obtained in other experiments are 163·2 and 121·6 s^{-1} for the control at +50 mV and 141·0 and 240·1 s^{-1} for 30 mM $[K^+]_o$ at +52 mV. Thus changing the external K^+ concentration affected both the blocking and the unblocking rate.

DISCUSSION

In this study, the effects of external and internal K^+ ions on the Mg^{2+} block of the inwardly rectifying K^+ channel were studied. The blocking efficacy of Mg^{2+} was hardly affected by changing the internal K^+ concentration, while it was increased by reducing the external K^+ concentration at a given voltage. The results may be expressed in a different way: the blocking effect of Mg^{2+} depends on voltage when E_K is shifted by changing internal K^+ and on driving force when E_K is shifted by changing external K^+. This is in accordance with findings in the inwardly rectifying K^+ channel of egg cells and skeletal muscle that inward rectification depends on driving force when E_K is altered by changing external K^+ and on voltage when E_K is altered by changing the internal K^+ (Hagiwara, Miyazaki & Rosenthal, 1976; Hagiwara & Yoshii, 1979; Hestrin, 1981; Leech & Stanfield, 1981).

It has been reported in other K^+ channels that the blocking effect of internal cations is decreased by increasing external K^+: in Na^+ block of the Ca^{2+}-activated K^+ channel of bovine chromaffin cells (Marty, 1983; Yellen, 1984) and Mg^{2+} block of the ATP-regulated K^+ channel of guinea-pig ventricular cells (Horie *et al.* 1987). Such an effect of K^+ ions added to the side of the membrane opposite to the blocker has been ascribed to speeding the exit of a blocker from the channel (Yellen, 1984; Horie *et al.* 1987). In this study, both the blocking and unblocking rates were affected by external K^+, suggesting that both competition between Mg^{2+} and K^+ for binding to the site and unblock induced by K^+ occur.

Effects of external K^+ ions have been examined on the block by external cations of the inward current through the inwardly rectifying K^+ channel. The block by external Ba^{2+} and Sr^{2+} was not affected by external K^+ in egg cells (Hagiwara, Miyazaki, Moody & Patlak, 1978; Ohmori, 1980), while the block by external Ba^{2+} was increased by reducing external K^+ in skeletal muscle (Standen & Stanfield, 1978). Potentiation of the blocking effect of a monovalent cation such as Cs^+ or Na^+ by increasing external K^+ (but decrease of Na^+ block by K^+ at concentrations higher than 20 mM) has been noted in egg cells and skeletal muscle (Hagiwara *et al.* 1976; Ohmori, 1980; Fukushima, 1982; Senyk, 1986). This result has been explained by a two-site multi-ion model (Ciani, Krasne & Hagiwara, 1980; Ohmori, 1980; Senyk, 1986).

The present results are also considered in terms of the multi-ion single-file pore model described by Hille & Schwarz (1978). It is considered here that the conducting unit has two energy minima (sites or wells) that can either be empty or can contain an ion. Ions move from one site to an adjacent empty site over an intervening energy maximum (barrier). Both sites may be filled simultaneously. The voltage dependence of the dissociation constant gave a value for the fractional electrical distance of the Mg^{2+} binding site of 0·57. For modelling, I have arbitrarily assumed that the two sites are located at electrical distances of 0·3 and 0·6 from the internal mouth and that only the outer site has a high affinity for Mg^{2+}. It is also supposed that Mg^{2+} can cross the inner and middle barriers of the pore but cannot cross the outer barrier. Peaks of the three barriers are assumed to be located at 0·15, 0·45 and 0·8 from the internal mouth of the pore.

With two sites and two types of ions, there are nine possible states for the pore. On the assumption that Mg^{2+} ions exist inside the cell and cannot pass the outer barrier, twenty-two (eleven forward and eleven reverse) rate constants derived from rate theory connect these states (see the diagram shown in Fig. 2*C* of Hille & Schwarz, 1978). Entry rate constants include the ionic concentrations. The steady-state probability of each state was calculated by the matrix method (Begenisich & Cahalan, 1980). After the rate constants and steady-state probabilities were obtained, the steady-state K^+ flux was calculated as the net rate of K^+ ions crossing the middle barrier. Normalized currents were obtained by dividing the steady-state K^+ flux in the presence of Mg^{2+} by that in the absence of Mg^{2+}.

In a three-site model with a monovalent internal blocking ion, Hille & Schwarz (1978) successfully simulated inward rectification that depended on driving force at different external K^+ concentrations. They also pointed out that when the blocking ion is divalent the block shifts much less than the change in E_K caused by changing external K^+. In my calculation the shift of the Mg^{2+} block was less than 20 mV when reducing external K^+ from 150 mM to 30 mM shifted the zero-current potential by some 40 mV. Taking into account that the K_D at 0 mV is dependent on the external K^+ concentration (37 μM for the control and 45 mM $[K^+]_i$ and 8·8 μM for 30 mM $[K^+]_o$), I have added another assumption to reconcile the experimental results. If it is assumed that the energy of Mg^{2+} bound to the site in an otherwise empty pore is given by (Almers & McCleskey, 1984):

$$\Delta G_W = RT \ln K_D(0),$$

and that the energy of Mg^{2+} bound to the site is affected by external K^+, the shift of the block observed in the experiments can be simulated. The curves in the upper panel of Fig. 5*B* show normalized current–voltage relations in the presence of 2 μM-

Mg^{2+} using the above assumption and the following variables: the energy barriers for K^+ (from exterior to interior) are $8RT$, $4RT$ and $8RT$, and for Mg^{2+} ions are $4RT$ (middle) and $8RT$ (interior); the energy wells for K^+ are $-2{\cdot}5RT$ and $-2{\cdot}5RT$ and for Mg^{2+} are $-10{\cdot}2RT$ (exterior) (and $-11{\cdot}6RT$ with 30 mM $[K^+]_o$) and $-2{\cdot}5RT$ (interior). It can be seen that the model gives a fairly good fit to the experimental results. (Because repulsion between ions incorporated according to Hille & Schwarz (1978) and Hess & Tsien (1984) predicts the block at more positive potentials, it was excluded.) In considering the effect of internal K^+, internal K^+ may not only compete with Mg^{2+} for binding to the site to decrease block but also lock Mg^{2+} in the outer well to increase block, resulting in a small change in the block with reduction from 155 mM to 45 mM.

The appearance, when the channel is open, of four equally spaced conductance levels (including the zero-current level) suggests that the cardiac inwardly rectifying K^+ channel consists of three identical conducting units that function co-operatively to form a single channel and that Mg^{2+} may enter and plug up each subunit to produce the substate behaviour seen at positive potentials. In terms of the binomial model, five measurable quantities, τ_0, τ_1, τ_2, τ_3 and p, yield calculations of two rate constants, λ and μ. This allows the validity of the binomial model to be tested by calculating the rate constants from some of the measurements and comparing the other experimental values with the values calculated using the rate constants. Calculated time constants, τ_0, τ_1 and τ_3, for the examples shown in Fig. 8 are 1·86, 2·04 and 2·55 ms for *A*, and 2·72, 1·83 and 1·11 ms for *B*. Agreement between the observed and predicted values was not so good as in Cs^+ and Rb^+ block (Matsuda *et al.* 1989). This may imply some co-operative interactions between subunits during Mg^{2+} block. However, in the present study, no further analysis was done on this point and a conducting unit was treated as an independent pore to be blocked by one Mg^{2+} ion.

I thank Drs N. B. Standen and A. M. Frace for comments on the manuscript. This work was supported by a grant from the Ministry of Education, Science and Culture of Japan.

REFERENCES

Almers, W. & McCleskey, E. W. (1984). Non-selective conductance in calcium channels of frog muscle: calcium selectivity in a single-file pore. *Journal of Physiology* **353**, 585–608.

Begenisich, T. B. & Cahalan, M. D. (1980). Sodium channel permeation in squid axons. I: Reversal potential experiments. *Journal of Physiology* **307**, 217–242.

Ciani, S., Krasne, S. & Hagiwara, S. (1980). A model for the effects of potential and external K^+ concentration on the Cs^+ blocking of inward rectification. *Biophysical Journal* **30**, 199–204.

Fabiato, A. & Fabiato, F. (1979). Calculator programs for computing the composition of the solutions containing multiple metals and ligands used for experiments in skinned muscle cells. *Journal de Physiologie* **75**, 463–505.

Findlay, I. (1987). ATP-sensitive K^+ channels in rat ventricular myocytes are blocked and inactivated by internal divalent cations. *Pflügers Archiv* **410**, 313–320.

Fukushima, Y. (1982). Blocking kinetics of the anomalous potassium rectifier of tunicate egg studied by single channel recording. *Journal of Physiology* **331**, 311–331.

Hagiwara, S., Miyazaki, S., Moody, W. & Patlak, J. (1978). Blocking effects of barium and hydrogen ions on the potassium current during anomalous rectification in the starfish egg. *Journal of Physiology* **279**, 167–185.

HAGIWARA, S., MIYAZAKI, S. & ROSENTHAL, N. P. (1976). Potassium current and the effect of cesium on this current during anomalous rectification of the egg cell membrane of a starfish. *Journal of General Physiology* **67**, 621–638.

HAGIWARA, S. & YOSHII, M. (1979). Effects of internal potassium and sodium on the anomalous rectification of the starfish egg as examined by internal perfusion. *Journal of Physiology* **292**, 251–265.

HAMILL, O. P., MARTY, A., NEHER, E., SAKMANN, B. & SIGWORTH, F. J. (1981). Improved patch-clamp techniques for high-resolution current recording from cells and cell-free membrane patches. *Pflügers Archiv* **391**, 85–100.

HESS, P. & TSIEN, R. W. (1984). Mechanism of ion permeation through calcium channels. *Nature* **309**, 453–456.

HESTRIN, S. (1981). The interaction of potassium with the activation of anomalous rectification in frog muscle membrane. *Journal of Physiology* **317**, 497–508.

HILLE, B. & SCHWARZ, W. (1978). Potassium channels as multi-ion single-file pores. *Journal of General Physiology* **72**, 409–442.

HORIE, M. & IRISAWA, H. (1987). Rectification of muscarinic K^+ current by magnesium ion in guinea pig atrial cells. *American Journal of Physiology* **253**, H210–214.

HORIE, M. & IRISAWA, H. (1989). Dual effects of intracellular magnesium on muscarinic potassium channel current in single guinea-pig atrial cells. *Journal of Physiology* **408**, 313–332.

HORIE, M., IRISAWA, H. & NOMA, A. (1987). Voltage-dependent magnesium block of adenosine-triphosphate-sensitive potassium channel in guinea-pig ventricular cells. *Journal of Physiology* **387**, 251–272.

KATZ, B. (1949). Les constantes électriques de la membrane du muscle. *Archives des Sciences Physiologiques* **3**, 285–300.

LEECH, C. A. & STANFIELD, P. R. (1981). Inward rectification in frog skeletal muscle fibres and its dependence on membrane potential and external potassium. *Journal of Physiology* **319**, 295–309.

MARTY, A. (1983). Blocking of large unitary calcium-dependent potassium currents by internal sodium ions. *Pflügers Archiv* **396**, 179–181.

MATSUDA, H. (1988). Open-state substructure of inwardly rectifying potassium channels revealed by magnesium block in guinea-pig heart cells. *Journal of Physiology* **397**, 237–258.

MATSUDA, H., MATSUURA, H. & NOMA, A (1989). Triple-barrel structure of inwardly rectifying K^+ channels revealed by Cs^+ and Rb^+ block in guinea-pig heart cells. *Journal of Physiology* **413**, 139–157.

MATSUDA, H., SAIGUSA, A. & IRISAWA, H. (1987). Ohmic conductance through the inwardly rectifying K channel and blocking by internal Mg^{2+}. *Nature* **325**, 156–159.

MATSUDA, H. & STANFIELD, P. R. (1989). Single inwardly rectifying potassium channels in cultured muscle cells from rat and mouse. *Journal of Physiology* **414**, 111–124.

OHMORI, H. (1980). Dual effects of K ions upon the inactivation of the anomalous rectifier of the tunicate egg cell membrane. *Journal of Membrane Biology* **53**, 143–156.

SAKMANN, B. & TRUBE, G. (1984). Conductance properties of single inwardly rectifying potassium channels in ventricular cells from guinea-pig heart. *Journal of Physiology* **347**, 641–657.

SENYK, O. (1986). External $[K^+]$ and the block of the K^+ inward rectifier by external Cs^+ in frog skeletal muscle. *Biophysical Journal* **50**, 677–683.

STANDEN, N. B. & STANFIELD, P. R. (1978). A potential- and time-dependent blockade of inward rectification in frog skeletal muscle fibres by barium and strontium ions. *Journal of Physiology* **280**, 169–191.

TSIEN, R. Y. & RINK, T. J. (1980). Neutral carrier ion-selective microelectrodes for measurement of intracellular free calcium. *Biochimica et Biophysica Acta* **599**, 623–638.

VANDENBERG, C. A. (1987). Inward rectification of a potassium channel in cardiac ventricular cells depends on internal magnesium ions. *Proceedings of the National Academy of Sciences of the USA* **84**, 2560–2564.

WANG, Z., KIMITSUKI, T. & NOMA, A. (1991). Conductance properties of the Na^+-activated K^+ channel in guinea-pig ventricular cells. *Journal of Physiology* **433**, 241–257.

WOODHULL, A. M. (1973). Ionic blockage of sodium channels in nerve. *Journal of General Physiology* **61**, 687–708.

YELLEN, G. (1984). Relief of Na^+ block of Ca^{2+}-activated K^+ channels by external cations. *Journal of General Physiology* **84**, 187–199.